# Glial Associated Impairment of the Glymphatic System in Experimental Neonatal Hydrocephalus

**Joseph Tyler Vasas** ( vasasj@musc.edu )
Medical University of South Carolina College of Medicine https://orcid.org/0000-0002-0818-0830
**James Pat McAllister**
Washington University School of Medicine in Saint Louis: Washington University in St Louis School of Medicine
**Ramin Eskandari**
MUSC: Medical University of South Carolina Department of Neurosurgery

**Research**

**Keywords:** Glymphatics, Chronic, Neonatal, Hydrocephalus, Aquaporin-4, Gliosis, Brain Injury

**Posted Date:** January 8th, 2021

**DOI:** https://doi.org/10.21203/rs.3.rs-139923/v1

## Abstract

# Background

Changes in aquaporin-4 (AQP4) and glial fibrillary acid protein (GFAP) expression by astrocytes have been observed in several pathologies. It is hypothesized that prolonged exposure to pathologically elevated intracranial pressure (ICP) may be linked to impaired glymphatic pathways. In this study we explore histological consequences of prolonged pressure-induced injury in a feline model of neonatal hydrocephalus through changes in AQP4 and GFAP expression. We discuss the implications this may have in gaining a better understanding of the underlying mechanisms of hydrocephalus (HCP).

# Methods

Using a neonatal feline model, obstructive HCP was induced through kaolin injection into the cisterna magna. Time between injection and intervention via ventricular reservoir placement was used to divide groups into early and late treatment groups. Early and late animals received reservoirs at 1- and 2-weeks post kaolin injection, respectively. Controls underwent sham operations (saline injection instead of kaolin). Animals were sacrificed at 4 months allowing for a chronic treated hydrocephalic model at time of brain harvest. Immunofluorescent staining for GFAP, AQP4 and DAPI was performed on histological brain sections from each group, and densitometry was used to quantify the relative signal of protein expression.

# Results

Hydrocephalus was seen in all animals receiving kaolin injection as demonstrated by magnetic resonance imaging, clinical examination and neurological sequelae. Hydrocephalic animals demonstrated lower levels of perivascular AQP4 expression, increased diffuse AQP4 expression and increased glial scarring of perivascular, ependymal and subependymal spaces. Cerebral microvasculature of early treatment groups demonstrated increased astrocytic processes in the perivascular spaces, while late treatment groups demonstrated increased glial scar formation. Overall, the glymphatic system was severely disrupted in chronic treated hydrocephalus compared to controls.

# Conclusions

Reactive astrogliosis and AQP4 mislocation are evident in early and late reservoir-treated HCP. Glial scarring in the perivascular, ependymal and subependymal spaces concurrent with AQP4 internalization from the perivascular region are prominent in HCP conditions present within the neonatal period. Delay in treatment by 1 week demonstrates quantifiable increases in perivascular and ependymal glial scarring at

4 months of age. Further investigation is needed to correlate glymphatic disruption with impaired CSF absorption and its role in promoting progressive hydrocephalus.

# Background

The incidence of pediatric hydrocephalus (HCP) peaks in the first two years of life. Timing of diagnosis and treatment remain the most varied in neurosurgical practice, placing neonates at the highest risk for disease progression, delayed treatment and poor disease management (1, 2). An estimated 400,000 new cases of pediatric HCP develop each year, and while surgical remedies do exist, hardware malfunction and infection rates carry significant safety and economic burdens costing over $2 billion annually in the United States alone (3, 4). Early injury from hydrocephalus may leave affected children with lifelong neurological impairment and caretaker dependency (3). Premature infants, many of whom develop HCP after intracranial hemorrhage, frequently spend extended periods in intensive care, requiring chronic cerebrospinal fluid (CSF) diversion to mitigate the effects of progressive HCP. These babies are often temporized by implantation of ventricular access devices (i.e. reservoirs) which aid in chronic periods of CSF removal (5, 6), however the pathophysiology of cerebrospinal fluid flow in this vulnerable population remains elusive, as some patients go on to require permanent CSF diversion while others manage to regain physiologic CSF equilibrium.

Characterization of the glymphatic system has broadened the scope of HCP research by questioning the existence of alternative pathways for CSF production and absorption. Evidence from neurodegenerative diseases such as Alzheimer's Disease postulate glymphatic involvement in accumulation of central nervous system (CNS) waste such as amyloid-ß and tau protein (7). The glymphatic system's function as it pertains to hydrocephalus, specifically within the neonatal population, remains a novel but promising field of research. As such, evidence continues to implicate the critical roles that glymphatic structures play in CNS waste-management, CSF homeostasis, and nutrient delivery (4, 7, 8). As demonstrated by Iliff et al., CSF is first localized around arteries within the subarachnoid space, including smaller vessels that penetrate deep into cortex by way of perforating arterioles and through deep sulcal folds. Eventually, CSF occupies the paravascular spaces (PVS) of capillaries, a region within which the contribution toward clearance of CSF, movement of water and removal of waste products continues to be debated heavily. Polarized to the endfeet of astrocytes, aquaporin-4 (AQP4) is a transmembrane channel that facilitates water flux across intracellular, interstitial and paravascular spaces (9-11). To better understand the pathophysiology of neonatal HCP, we have examined astrocytic AQP4 to question its link between maintaining CNS fluid homeostasis and contributing to glymphatic function. Ultimately, CSF imbalance and thus water equilibrium within the cerebral ventricular system is a major pathophysiological driver of neonatal and pediatric HCP.

Currently the gap in knowledge characterizing AQP4 within brain glymphatics and neonatal brain injury from HCP remains wide. Our study evaluates both the microstructural and morphological changes occurring across multiple regions of brain using our previously described neonatal model of chronic reservoir-treated neonatal HCP(12). With these findings we hope to begin bridging the gap between the

pathophysiology of AQP4 and the glymphatic system in HCP while opening the door for potential targeted therapeutics directed at these new injury mechanisms.

# Methods

All tissue utilized in this study was formalin-fixed and obtained via an experimental feline design (Supplemental Figure 1) described in detail by Eskandari et al. (12). Animals were separated into 3 cohorts of control (n = 2), early-treatment (n = 3) and late-treatment (n = 3). In brief, hydrocephalus was induced in the treatment groups within the kittens' first week of life by kaolin injections into the cisterna magna. Treatment groups received intraventricular catheters connected to Ommaya reservoirs to enable intermittent treatment via percutaneous tapping of the reservoir. Prerequisites for inclusion in the early group were MRI demonstration of ventriculomegaly *without* significant clinical signs of elevated ICP [12]. The late-treatment group demonstrated both radiographic and clinical signs of elevated ICP. Early- and late-groups were treated with ventricular catheters and reservoirs at 5-7 and 12-14 days post-kaolin, respectively. Control animals underwent intracisternal sham injections of saline at the same volume as kaolin. All groups were followed with routine MRI and daily clinical assessment scores which guided reservoir tapping, until sacrifice at 4 months of age.

*Sectioning*: Each brain was divided into coronal blocks (frontal, parietal, and occipital), and each block was processed and embedded in paraffin. Paraffin-embedded cortex was sectioned serially at 10μm using a Reichert-Jung 2030 rotary microtome (Microm-Zeiss, Jena, Germany). Sections were float-mounted onto subbed glass slides (Ted Pella, Inc., Redding, California) and incubated at 37$^{o}$C overnight.

*Immunohistochemistry*: Using standard immunohistochemistry procedures, sections were deparaffinized, rehydrated and underwent heat-induced epitope retrieval. Antigen retrieval was performed by submerging the sections into a heated citrate buffer antigen unmasking solution (Vector Laboratories, Burlingame, CA) followed by 25 min steam-incubation. Following antigen retrieval, slides were left to cool. A hydrophobic barrier (Vector Laboratories, Burlingame, CA) was used to encircle the mounted tissue. A blocking mixture with 10% normal donkey serum (NDS), 3% bovine serum albumin (BSA) in 1X PBS-T was applied to sections and left to incubate at room temperature for 90 minutes. Next, the blocking serum was gently aspirated and an optimized primary antibody dilution (3% NDS, 1% BSA, a 1X PBS-T solvent, and compatible primary antibodies) was applied to sections and incubated for 20hrs at 4$^{o}$C. Primary antibodies: monoclonal mouse anti-GFAP (1:1000; Invitrogen, MA1-19170), monoclonal rabbit anti-AQP4 (1:1000; Cell Signaling, 59678).

Following primary incubation, the primary antibody mixture was first aspirated and then rinsed from sections with 1X PBS. The secondary antibody mixture, consisting of 3% NDS, 1% BSA and compatible secondary antibodies (donkey anti-rabbit AF-488, donkey anti-mouse AF-555) were mixed at a 1:500 dilution, applied to sections and incubated at room temperature for 1.5 hrs guarded from light. The secondary antibody mixture was then rinsed, and sections were cover-slipped with a fluorescent mounting medium (Thermo Fisher Scientific, Waltham, MA) including a DAPI cell body stain.

*Tissue Analysis:* All images were obtained by an individual researcher on a fluorescent microscope Keyence BZ-X710 (Keyence, Itasca, IL). Photomicrographs were obtained from representative cortical and subcortical structures using methods similar to those recently published by Ding and colleagues (13).

*Image Analysis:* Quantitative and qualitative image analysis was conducted blindly by importing images from microscopy into ImageJ (National Institutes of Health and the Laboratory for Optical and Computational Instrumentation - LOCI, University of Wisconsin). Quantitative analysis was performed by a single research technician trained in this software. Computerized image-capture was performed using a minimum of 6 representative sets of non-overlapping images per designated brain region. Four representative brain regions were collected; Superficial Cortex (SC), Deep Cortex (DC), Periventricular (PV) and Deep White Matter (DWM) (Fig. 1). Densitometry measurements were acquired using Image J software.

*Statistical Analysis:* Differences in densitometry measurements were compared using the Mann-Whitney test with Bonferroni's test for multiple comparisons (Prism, Graph Pad Software, La Jolla, CA). Repeated measures were used when comparing the results obtained from histological images depicting GFAP and AQP4. Data are reported as mean values $\pm$ the standard error of the mean. P-values $<0.05$ were considered statistically significant between brain regions and between experimental groups.

# Results

### Control Animals

Deep white matter (DWM) demonstrated the highest levels of GFAP and AQP4 expression, significantly higher than deep cortex (DC; 193%, p = 0.0022, GFAP) (146%, p = 0.0043, AQP4) and superficial cortex (SC; 74%, p = 0.0043, GFAP) (48%, p =0.3939, AQP4) regions (Fig2A,D,G; Fig. 3A-D). Furthermore, both SC GFAP and AQP4 were significantly higher than within the DC (184%, p = 0.0022, GFAP) (118%, p = 0.0043, AQP4). Periventricular regions (PV) also exhibited significantly higher mean levels of GFAP and AQP4 than did the DC region (187%, p = 0.0022, GFAP) (84%, p = 0.0260). While the expression of SC AQP4 remained slightly higher than levels observed within PV regions (45%, p = 0.0411), the opposite was true for GFAP in this region (20%, p = 0.1320).

Summary of control animal findings: AQP4 levels highest in DWM>>>PC>PV=ST. GFAP levels highest in DWM>>>PC=PV>ST.

### GFAP Cytology in Control and Hydrocephalic Animals

Qualitative analysis of GFAP expression revealed visible differences between experimental cohorts. As baseline for comparison of astrocytic morphology in qualitative analysis, control animals exhibited non-reactive astrocyte morphology with GFAP+ staining ; fibrous astrocytes in the PV white matter maintained elongated cell bodies while stellate cortical astrocytes exhibited round cell bodies(14). In control animals, both subtypes of astrocytes extended thin, morphologically non-reactive GFAP+ processes with endfeet

against capillaries and deep parenchymal paravascular at times exceeding 60μm (Fig. 2A, D, G). In contrast, astrocytes within both early and late-treated chronically hydrocephalic tissue demonstrated marked *reactive* morphology with changes noted most prominently in late-treated animals. Brain regions in early-treated animals demonstrated more reactive astrocytes with thicker, shorter processes and loss of homogeneity in their cell bodies compared with controls (Fig. 2B, E, H). Careful inspection revealed both reactive and non-reactive processes surrounding DC vasculature of the early-treated animals (Fig. 2 – E, H). Brain regions in the late-treated animals are visibly altered compared to both control and early groups. Overall discernable astrocyte cell bodies or processes are lacking, while thick GFAP+ “plaques” are instead plentiful. These plaques, or glial scars, are most prevalent within the DC, surrounding the vasculature of the late-treated brains (Fig. 2C, F, I).

### GFAP by Brain Region – Within Cohort Quantitative Comparison

Expression of GFAP within early-treated animals demonstrated significantly higher levels within the DWM as compared to DC (197%, p = 0.0286) as well as the SC region (118%, p = 0.0286), similar to control group animals (Fig. 3). Although statistical significance was not reached, DWM GFAP expression was also higher than levels measured within the periventricular regions (83%, p = 0.0571). Again, similar to control animals, GFAP expression in late-treated animals remained highest within DWM, with significantly more expression occurring over DC (194%, p = 0.0014) and SC (166%, p = 0.0256) regions. Additionally, all animals exhibited a relative paucity of GFAP within regions of DC (Fig. 3C, G, K). However, while late-treated animals demonstrate an overall decrease in levels of GFAP expression, the large difference in GFAP expression that was previously observed between the PV and DC regions within control and early-treatment groups diminishes (Fig. 3J and K).

### GFAP by Brain Region – Between Cohort Quantitative Comparison

Comparisons between experimental groups revealed SC regions of late-treated animals to have a significantly lower mean GFAP expression than control (84%, p = 0.0022) and early-treated (77%, p = 0.0190) animals (Fig. 3). Likewise, PV regions of the late-treated cohort demonstrated significantly lower GFAP than control (70%, p = 0.0152) and early-treated (68%, p = 0.0381) animals. Regional GFAP expression was decreased in all late-treated animals relative to controls. Additionally, all ROIs (aside from DC) within late-treated animals demonstrated a decrease in mean GFAP expression in comparison to their early-treated counterparts. Notably, the decrease in GFAP expression appeared to be particularly prominent within the SC region in comparison to other ROIs. Overall, we noted a distinct decrease in GFAP signal in the brains of late-treated animals compared with control and early-treated cohorts.

### AQP4 Cytology in Control and Hydrocephalic Animals

Qualitative observations revealed conspicuous regional variability in AQP4 expression within the paravascular sheath surrounding much of the brain’s microvasculature (Fig. 4). Superficial cortex AQP4 immunostaining in control tissue demonstrated very little localization in regions other than those which immediately bordered vessel walls (Fig. 5A). In contrast, SC regions in early-treated animals exhibited

lower perivascular AQP4 signal and increased nonspecific signal throughout tissue distant from vasculature (Fig. 5B).

Qualitative differences showed that AQP4 expression between control and early-treated animals was substantially more profound in PV regions compared to SC (Fig. 4). Within the DC, there was relative paucity of AQP4 staining in both control and early-treated animals, whereas the late group demonstrated visible increase in signal. Deep white matter AQP4 signal was relatively consistent in the control, early and late groups, however, AQP4 adjacent to more superficial white matter structures was much more prominent (Fig. 4 – D, H, L). Noteworthy within both the DC and DWM regions was the pattern of diminished paravascular AQP4 localization and more diffuse non-specific AQP4 signal in early and more prominently in late treatment animals compared with controls.

### AQP4 by Brain Region – Within Cohort Quantitative Comparison

As with GFAP, differences in regional AQP4 expression were assessed within each cohort. In early-treated animals AQP4 was significantly higher within DWM compared to both DC (140%, $p = 0.0286$), and periventricular (145%, $p = 0.0286$) regions (Fig. 4). Late-treated animals demonstrated both significant SC (162%, $p = 0.0022$) and periventricular (193%, $p = 0.0022$) decline in AQP4 expression relative to DWM. Furthermore, AQP4 expression increased within regions of DC in the late-treated group and was significantly different compared to the periventricular region (178%, $p = 0.0022$).

### AQP4 by Brain Region – Between Cohort Quantitative Comparison

Superficial cortex AQP4 was significantly decreased in the late-treated group relative to both control (82%, $p = 0.0022$) and early-treated (79%, $p = 0.0190$) animals (Fig. 4). Similar, but more profound decline in AQP4 was demonstrated in the PV region of late-treated animals compared with control (95%, $p = 0.0022$) and early-treated animals (88%, $p = 0.0381$). Most notable, however, was the increase in DC AQP4 expression between control and late-treated groups. Unlike the relative paucity of GFAP found within the DC of all three experimental groups, AQP4 signal nearly doubled within the DC of late-treated animals as compared to controls (108%, $p = 0.0260$) and early-treated animals (86%, $p = 0.2571$). AQP4 density within the DWM did not change between experimental cohorts. Similar staining patterns to that of GFAP were observed for AQP4 in both the SC and PV regions (Fig. 4 – AQP4 and Fig. 5 – GFAP) Overall, we noted AQP4 expression shifting from the SC and PV regions in control and early-treated animals, toward DC and DWM labeling in those treated late with ventricular reservoirs.

## Discussion

In this study, non-hydrocephalic controls demonstrated that GFAP expression was highest within deep white matter regions, lowest within the deep cortex, and was slightly higher within periventricular regions in comparison to those which were superficial cortex. Similar relative differences were demonstrated by AQP4 expression within controls, the only difference being that slightly higher levels of AQP4 expression were detected within superficial cortex compared to periventricular locations. Histological analysis

demonstrated that a delay in treatment time resulted in significant decreases in GFAP expression in SC and PV regions compared to controls after chronically treated hydrocephalus. Similar patterns were observed in AQP4 expression where late treated animals demonstrated significant decreases in AQP4 expression within SC and PV regions compared to controls, while DWM remained stable. Interestingly, unlike GFAP, AQP4 expression within DC exhibited a significant increase. Our findings demonstrate that within the brains of hydrocephalic neonatal felines, a significant redistribution of GFAP and AQP4 occurs in a region dependent manner. Since these changes are localized to specific paravascular sites, our results support an involvement of an impaired glymphatic system within the hydrocephalic brain.

Expression of key glymphatic biomarkers, GFAP and AQP4, were altered significantly in our model of chronic neonatal hydrocephalus. Although our group and others have employed experimental models of delayed shunting and non-treated hydrocephalus in (14-16), to the best of our knowledge, this study is the first to follow chronic hydrocephalus for extended periods in a neonatal model and evaluate glymphatic disturbance in various treatment time points. Also important in analyzing the results of this study is the degree of ventricular enlargement which through the use of clinically indicated tapping criteria, demonstrated progressive increases in ventricular size without causing animal mortality. The degree of ventricular enlargement was similar to that seen in premature infants with post-hemorrhagic hydrocephalus(17, 18) and those born with congenital hydrocephalus (19, 20) who at times develop severe ventriculomegaly.

Control animals without hydrocephalus demonstrated GFAP expression that was highest within DWM regions (i.e. internal capsule), lowest within DC (deep cortical mantle along hemispheric convexity) and was higher within SC regions than PV regions. Control animals exhibited similar expression patterns in AQP4, the only difference being that AQP4 expression was slightly higher within periventricular vs SC regions. These baseline patterns demonstrated significant differences between brain regions but maintained ratios of GFAP/AQP4 which were similar among brain ROIs. Our chronic reservoir-treated hydrocephalus groups displayed surprising differences in the GFAP and AQP4 expression depending on the initial timing of reservoir treatment. Early-treated animals maintained relatively stable levels of GFAP throughout all brain ROIs without significant differences compared to controls. However, in late-treated animals, when signs of progressive hydrocephalus had fully developed in addition to grossly enlarged ventricles, GFAP levels were significantly altered at sacrifice 4 months later. Our a priori expectations were that GFAP and AQP4 levels may follow similar patterns in both treatment groups given the chronicity of the treatment timeline, however we noted a surprising *decrease* in overall GFAP expression in the late-treated animals in all ROIs with the greatest drop in SC and PV regions. By contrast, the levels of AQP4 in the DC of the late-treated animals doubled while SC and PV AQP4 dropped similar to that seen in the GFAP levels in the same cohort of late-treated animals. The overall drop in GFAP and rise in AQP4 in the DC demonstrated the first indication that the glymphatic unit of astrocyte endfeet, AQP4 water channels and perivascular spaces, were disrupted in chronically treated neonatal hydrocephalus.

Our previous studies have demonstrated a link between delayed reservoir treatment and larger ventricular volumes, altered DWM diffusion tensor imaging (DTI), neurological outcomes and decrease motor

accuracy scores (12, 21). It is noteworthy that once reservoirs were placed, the criteria for tapping was based on the *same* clinically-modeled assessment algorithm in both early and late treatment groups resulting in a typical tapping frequency of once or twice a day(12). Therefore, differences noted in the brains of early versus late animals can be traced to the decision to intervene before or after clinical signs of progressive hydrocephalus arise.

## Regional Differences

### Periventricular Region

The ependymal epithelium is both functionally and mechanically important to the developing neonatal CNS (22-24). Pioneering work by the Rodriquez and Jimenez laboratories have demonstrated ependymal denudation after experimental hydrocephalus, while Kahle and others have demonstrated a strong association between the functional unit of the normal ventricular ependyma with motile cilia and the maintenance of non-hydrocephalic states. These findings all demonstrate a critical role of ependymal cells facilitating normal CSF distribution (25-27). The single-cell ependymal layer also forms the physiologic boundary separating ventricular CSF from the developmentally important stem cells residing in the adjacent subventricular zone (28, 29). Ependymal injury from progressive ventricular dilatation compromises this fluid barrier exposing subependymal structures, including the PV glymphatic system to CSF.

We found that substantial decreases in PV AQP4 expression were present within both early and late treatment groups compared with control animals. Given that the early reservoir treated animals never developed clinical signs of significant ICP elevation but did have demonstrable ventricular enlargement on MRI, physical stress in the form of stretch injury to the ependymal lining and compressive injury to the immediate PV brain may have initiated an injury cascade permitting prolonged changes in glymphatic proteins at sacrifice. Our group and others have demonstrated that even short periods of time under pathological pressure can be detrimental to not only ependymal cilia, but also damage developing brain cells (12, 21, 30-38). When comparing the two treatment groups, late-treated animals demonstrated even more substantial decrease in AQP4 within the PV region, as well as significantly diminished GFAP signal in the same region, compared with early and control groups. In this model of neonatal hydrocephalus, investigation of early decisions can be longitudinally followed for durability and impact chronically. One explanation of these findings is that heightened vulnerability of PV cells, paired with disruption in CNS fluid homeostasis chronically facilitates an inflammatory cycle preventing full recovery in chronic progressive hydrocephalus.

Much like AQP4 within the CNS, GFAP is widely regarded as being expressed primarily by astrocytes, although its presence has been noted in immature ependymal cells (28, 39-41). While the primary function of GFAP is to maintain the structural integrity of astrocytes, this protein is also functionally important to the CNS immune response. Astrogliosis in response to cellular injury may be characterized

by increased astrocyte reactivity resulting in GFAP upregulation, changes in cell morphology and phenotypic polarization of astrocytes (42-47). Importantly, GFAP accumulation is integral in facilitating the physical isolation of damaged CNS tissue from viable tissue in adjacent regions (48-51). We found that while PV GFAP expression within the early treatment group was unchanged, within the late treatment group GFAP expression declined to one-third of non-hydrocephalic controls. We surmise that earlier intervention helped minimize cellular disturbances resulting in astrocyte preservation and increased neuronal viability immediately adjacent to the dilated ventricles. Polarization of perilesional astrocytes into a phenotypically reactive state is well-documented phenomenon after CNS injury (42, 45).

Therefore, it is reasonable that the loss of AQP4 on the endfeet of injured astrocytes may result from early injury *before* neurological deterioration or noticeable white matter degradation. We propose that the substantial decreases in both PV GFAP and AQP4 within the late treatment group could be due to astrocyte loss and glial scar formation. Late treatment animals demonstrated substantially thickened GFAP+ glial scars without identifiable astrocyte cell bodies or processes. Such scarring likely does not harbor functional components of the glymphatic unit and therefore can explain lack of AQP4+ water channels.

### Superficial Cortex Region

In the SC region, the effects of chronic HCP and ventriculomegaly resulted in diminished GFAP and AQP4 expression. However, unlike the significant decline in AQP4 observed in the PV region of both early and late treatment groups, AQP4 decrease within the SC region was only statistically significant in the late group, nearly one-fourth that seen in non-hydrocephalic controls. Notably, while AQP4 and GFAP levels within the PV and SC regions of the late treatment group seemed to decline proportionately relative to one another, a break in this pattern was observed in the expression of AQP4 with the PV region of early group. We reason that lower early group SC AQP4 loss compared with PV region could be partly due to relative anatomical positioning away from the expanding ventricles. As CSF accumulates within the ventricles from chronic hydrocephalus, the resulting injury mechanism may be simplified into two phases and may affect the PV regions differently compared with other CSF-containing regions of the brain (i.e. superficial subarachnoid, interstitial spaces etc.). Initially, as the ventricles enlarge, and the ependymal lining may give way to pressure, small gaps in the ventricular wall facilitates CSF exiting into the PV, and eventually DC regions of the brain. This pathological phenomenon demonstrated on most brain imaging is *transependymal flow* (52-54). Chronic hydrocephalus and sustained ventricular dilatation also facilitate compression injury of the cortical mantle against the rigid skull. These mechanisms are outlined by Del Bigio et. al. through work done on hydrocephalic rats, where MRI demonstrated focal, not diffuse changes in brain water content after kaolin-induced hydrocephalus in a neonatal model (55). We propose that with early HCP treatment (i.e. early reservoir treatment) before clinical signs of injury and significant cellular damage occurs, glymphatic units remained structurally intact longer maintaining closer to normal AQP4 levels within regions of the brain distant from the enlarged cerebral ventricles. Importantly, while the SC region seemed to offer a protective advantage in the early group, this anatomical advantage was nullified in the late group by delaying HCP treatment until pathological signs of disease became apparent through

worsening neurological deficit scores. Moreover, diffuse injury to cells within the PV and SC regions in the late group were likely from both chronic edema in the first phase of post-hydrocephalic injury, and chronic progressive compression against the hard surface skull in the second phase of injury. To some extent, this compressive injury may be dampened within the neonatal skull through its ability to expand due to open fontanelles and unfused sutures. However, the efficacy of these compensatory mechanisms diminishes as CSF accumulates, the ventricles expand and as ICP increases.

### Deep White Matter Regions

The internal capsule was used as representative DWM in our study. In previous studies, we and others have utilized many other white matter structures such as the crus cerebri, corpus callosum, optic nerves/chiasm/tracts and corona radiate (12, 21, 56). The decision to use deeper internal capsule fibers when comparing white matter to other structures such as the PV region, was to analyze a region that was relatively protected against direct ventricular pressure and anatomic distortion with severe thinning and compression against the rigid skull. Animals receiving reservoirs at the early treatment period demonstrated ventricular dilatation without clinical signs of elevated ICP, and our previous work concluded that internal capsule fibers were not as damaged by progressive hydrocephalus in the early treatment cohort through intact fractional anisotropy values and DTI (12, 21, 57). Histologically, neither GFAP nor AQP4 levels were significantly altered within the DWM of the early treatment group compared with controls. In the late treatment group, GFAP dropped compared with control and early treatment groups, yet AQP4 levels continued to increase. Although these trends did not achieve statistical significance, this may be secondary to low animal numbers and we believe deserves more attention in our future experiments. We may be witnessing that indeed DWM is partially protected during progressive hydrocephalus, however with chronicity and enough severity such as the late treatment groups, injuries in DWM regions are also possible.

Noteworthy is that our findings of DWM GFAP signal in progressive hydrocephalus are contrary to those found in neonatal HCP rats with congenital hydrocephalus, where reactive microglia were found predominantly in the crus cerebri and thalamic relay nuclei (56). Involvement of both microglia and astrocytes in neuroinflammation is well documented, and thus differences between these findings may be attributed to variation in cell specific activating factors such as timing, or differential expression in specific cellular phenotypes resulting from the injuries that accompany chronic HCP. However, given the discordant results, more detailed evaluation of DWM in pediatric hydrocephalus is needed.

The expression of GFAP and AQP4 within PV and SC regions seemed to follow a trend in which chronic injury led to decreased GFAP expression accompanied by proportional decreases in AQP4 expression in the early treatment group. Furthermore, increasing HCP severity from delayed treatment translated to further protein loss in the late treatment group. However, AQP4 within the DWM regions of both early and late treatment groups exhibited expression patterns which were opposite of those seen within PV and SC regions. Chronic HCP and ventriculomegaly resulted in increased DWM AQP4 expression in both early

and late treatment groups. Interestingly, delayed treatment resulted in further increases in DWM AQP4 expression.

### Deep Cortex Region

The DC region is composed of parenchyma deep to the gyral folds along the lateral convexity of the brain, containing neurons, superficial white matter and a paucity of astrocytes. Vasculature in this region is typically small arterioles, venules, and capillaries. Astrocytes within the DC demonstrate faint GFAP expression, tend to be protoplasmic subtype and lack extended processes (28, 58, 59). Baseline low GFAP expression made detection of differences between experimental groups challenging. Deep cortex AQP4 expression, however, demonstrated significant increase within the late treatment group, more than doubling compared with controls. While the mechanisms of AQP4 regulation are not fully understood, osmotic stress has recently been linked to overall AQP4 expression (60-62).

### Injury Mechanisms

Injury mechanisms in progressive hydrocephalus are multifactorial (i.e. stretch, compression, hypoxia/ischemia, edema, etc.) and often present simultaneously. Comparing injury between early and late reservoir groups highlights an important pathophysiology in chronic hydrocephalus; namely, significant decreases in AQP4 and GFAP within both the SC and PV regions of the late reservoir group, upregulation of DC AQP4, and mismatch between GFAP positive astrocytes and AQP4 water channels. Such derangements were not noted in the early treatment group, and thus we propose a threshold theory of early onset injury, below/before which progressive ventricular dilatation will not continue to cause harm. We have previously reported similar thresholds of injury using our model's Neurological Deficit Score (NDS) and ventricular volumes when evaluating potential white matter injury using DTI (57). In the first two-weeks after HCP induction, the rate of ventricular dilatation within the late treatment group was nearly twice that seen in the early treatment group secondary to earlier initiation of ventricular reservoir tapping. Since tapping criteria was held constant and clinically driven, ventricular volumes were monitored as a function of time and treatment group. Over time, the ventricular volumes in the early group slowly intersected that of the late group, and at sacrifice they were equivalent. Any histopathological differences seen in the brains of early versus late treatment groups is a function treatment timing during the first couple weeks of progressive hydrocephalus. With respect to essential glymphatic system constituents, treatment prior to obvious neurological deficits and signs of elevated ICP during critical neurodevelopmental periods facilitates histological outcomes (AQP4 and GFAP expression) that more closely resemble patterns in non-hydrocephalic controls.

One proposed mechanism of injury is that of early ependymal injury and subsequent consequences. Higher rates of ventricular dilatation early in development, paired with longer delays in treatment (late treatment group) resulted in more severe damage to the PV region, namely the ependymal epithelium. Delaying treatment also exposed these particular animals to longer periods of pathophysiological stress during developmentally critical times. We suspect that as a result of early damage to the ependymal lining compounded by subsequent chronic hydrocephalus-induced injury, flux of ventricular CSF into the

interstitial parenchyma diluted extracellular contents creating a state of extracellular hypotonicity. Previous studies have demonstrated the importance of AQP4 in astrocyte migration (61-63). Furthermore, they have demonstrated osmotic gradients to accelerate migration speed in the direction of the hypoosmotic region of the brain (64). If this fact holds true, then chronic hydrocephalus in the late treatment group would have caused a larger initial insult to the ependymal wall from more rapid increases of ventricular size and longer exposure to injurious conditions including pathological spread of CSF into the brain parenchyma from the ventricles toward the cortical surface. Moreover, continued chronic hydrocephalus causing stretch and compressive injury elevated levels of stress throughout the brain. To counteract these multiple injurious mechanisms, we see AQP4 is redirected into the regions of the brain with the largest total surface area for CSF removal, namely the DC capillaries. The decline of PV and SC AQP4 demonstrated only in the late group lends credibility to this potential pathophysiological mechanism.

# Limitations And Conclusions

The histopathological results in our study are highly consistent with findings in other models of chronic brain injury, although they challenge other long-held beliefs that GFAP upregulation is required in HCP-induced injury (65). Our findings of region-specific regulation of astrocytic proteins AQP4 and GFAP suggest that chronic hydrocephalus is accompanied by a redistribution of proteins known to be integral to glymphatic function. We intend to utilize these findings to gain deeper understanding of the underlying pathophysiological mechanisms characteristic of neonatal hydrocephalus. Furthermore, we intended to apply this knowledge in future experiments aimed at the identification of targeted treatment therapies for neonatal and pediatric hydrocephalus. This study faced several limitations, but none that would nullify findings which have led to several new testable hypotheses. In the future, we plan to mitigate our small numbers and limited focus on the two key glymphatic proteins AQP4 and GFAP by utilizing broader immunohistochemical targets such as neurons, oligodendrocytes, and microglia with larger animal cohorts. Furthermore, we were unable to definitively identify astrocytic subtypes due to inherent limitations present when utilizing GFAP alone as an astrocytic marker. Therefore, we plan to employ astrocytic markers such as S100Beta and NDRG2, to aid in quantifying the phenotypic variants of astrocytes present within the neonatal hydrocephalic brain. Furthermore, we plan to analyze the distribution of these variants as a function of age, hydrocephalus-mediated injury, and treatment-mediated recovery. Most importantly, we did not explore the many roles AQP4 plays in acute and chronic injuries. Recent research supports both positive and negative associations within the CNS when both GFAP and AQP4 deviate from physiological pattern of expression. We plan not only to explore the glymphatic-centered functionality of AQP4 and GFAP, but also their roles in cell migration, CNS waste management and immunity. A deeper understanding of these proteins is vital to the progression of glymphatic research aimed at identifying novel treatments for diseases with underlying glymphatic pathology.

# Abbreviations

GFAP – Glial Fibrillary Acid Protein

AQP4 – Aquaporin-4

CNS – Central Nervous System

CSF – Cerebrospinal Fluid

HCP – Hydrocephalus

MRI – Magnetic Resonance Imaging

ICP – Intracranial Pressure

BSA – Bovine Serum Albumin

NDS – Normal Donkey Serum

SC – Superficial Cortex

DC – Deep Cortex

PV – Periventricular

DWM – Deep White Matter

ROI – Region of Interest

DTI – Diffusion Tensor Imaging

NDS – Neurological Deficit Score

# Declarations

Ethics approval and consent to participate:

Animal care and protocols were all through approved IACUC protocols from the University of Utah DLAR (department of laboratory animal research). None of the animals were donated and all were bred for the purpose of research.

Consent for publication:

Not Applicable.

Availability of data and materials:

The datasets used and/or analyzed during the current study are available from the corresponding author on reasonable request.

Competing interests:

The authors declare that they have no competing interests.

Funding:

No funding was provided.

Authors' contributions:

TV made significant contributions to all immunohistochemical procedures, all data acquisition, analysis and interpretation, and has drafted and revised significant portions of this manuscript. RE made significant contributions to data analysis and interpretation, and has drafted and revised significant portions of this manuscript. PM made significant contributions to the drafting and revision of this manuscript. All authors read and approved of the final manuscript.

Acknowledgements:

Not Applicable.

**Disclosure of Funding**: There was no funding received for this study.

**Previous Presentations**:

This work was previously presented at the national AANS/CNS pediatrics section in 2019. Reference below:

Vasas T, Eskandari R, McAllister JP, “Glial Associated Impairment of the Glymphatic System”, AANS/CNS Section of Pediatric Neurological Surgery Meeting. December 6, 2019. Scottsdale, AZ. Abstract. [Oral Presentation].

# References

1. Vinchon M, Rekate H, Kulkarni AV. Pediatric hydrocephalus outcomes: a review. Fluids and barriers of the CNS. 2012;9(1):18.
2. Vinchon M, Baroncini M, Delestret I. Adult outcome of pediatric hydrocephalus. Childs Nerv Syst. 2012;28(6):847-54.
3. Riva-Cambrin J, Shannon CN, Holubkov R, Whitehead WE, Kulkarni AV, Drake J, et al. Center effect and other factors influencing temporization and shunting of cerebrospinal fluid in preterm infants with intraventricular hemorrhage. J Neurosurg Pediatr. 2012;9(5):473-81.

4. Dewan MC, Rattani A, Mekary R, Glancz LJ, Yunusa I, Baticulon RE, et al. Global hydrocephalus epidemiology and incidence: systematic review and meta-analysis. J Neurosurg. 2018:1-15.
5. Flanders TM, Kimmel AC, Lang SS, Bellah R, Chuo J, Wellons JC, 3rd, et al. Standardizing treatment of preterm infants with post-hemorrhagic hydrocephalus at a single institution with a multidisciplinary team. Childs Nerv Syst. 2020;36(8):1737-44.
6. Wellons JC, 3rd, Shannon CN, Holubkov R, Riva-Cambrin J, Kulkarni AV, Limbrick DD, Jr., et al. Shunting outcomes in posthemorrhagic hydrocephalus: results of a Hydrocephalus Clinical Research Network prospective cohort study. J Neurosurg Pediatr. 2017;20(1):19-29.
7. Iliff JJ, Wang M, Liao Y, Plogg BA, Peng W, Gundersen GA, et al. A paravascular pathway facilitates CSF flow through the brain parenchyma and the clearance of interstitial solutes, including amyloid β. Sci Transl Med. 2012;4(147):147ra11.
8. Da Mesquita S, Fu Z, Kipnis J. The Meningeal Lymphatic System: A New Player in Neurophysiology. Neuron. 2018;100(2):375-88.
9. Shchepareva ME, Zakharova MN. Functional Role of Aquaporins in the Nervous System under Normal and Pathological Conditions. Neurochemical Journal. 2020;14:1-8.
10. Arighi A, Di Cristofori A, Fenoglio C, Borsa S, D'Anca M, Fumagalli GG, et al. Cerebrospinal Fluid Level of Aquaporin4: A New Window on Glymphatic System Involvement in Neurodegenerative Disease? Journal of Alzheimer's disease : JAD. 2019;69(3):663-9.
11. Nakada T, Kwee IL. Fluid Dynamics Inside the Brain Barrier: Current Concept of Interstitial Flow, Glymphatic Flow, and Cerebrospinal Fluid Circulation in the Brain. Neuroscientist. 2018;Epub ahead of print:1073858418775027.
12. Eskandari R, Packer M, Burdett EC, McAllister JP, 2nd. Effect of delayed intermittent ventricular drainage on ventriculomegaly and neurological deficits in experimental neonatal hydrocephalus. Childs Nerv Syst. 2012;28(11):1849-61.
13. Ding Y, Zhang T, Wu G, McBride DW, Xu N, Klebe DW, et al. Astrogliosis inhibition attenuates hydrocephalus by increasing cerebrospinal fluid reabsorption through the glymphatic system after germinal matrix hemorrhage running title: Glymphatic system and hydrocephalus. Exp Neurol. 2019:113003.
14. Miller JM, McAllister JP, 2nd. Reduction of astrogliosis and microgliosis by cerebrospinal fluid shunting in experimental hydrocephalus. Cerebrospinal Fluid Res. 2007;4:5.
15. Lackner P, Vahmjanin A, Hu Q, Krafft PR, Rolland W, Zhang JH. Chronic hydrocephalus after experimental subarachnoid hemorrhage. PLoS One. 2013;8(7):e69571.
16. Li J, McAllister JP, 2nd, Shen Y, Wagshul ME, Miller JM, Egnor MR, et al. Communicating hydrocephalus in adult rats with kaolin obstruction of the basal cisterns or the cortical subarachnoid space. Exp Neurol. 2008;211(2):351-61.
17. Borenstein-Levin L, Makhoul S, Ilivitzki A, Zreik M, Hochwald O, Makhoul JS, et al. Neonatal frontal lobe: sonographic reference values and suggested clinical use. Pediatr Res. 2020;87(3):536-40.

18. Qiu W, Yuan J, Rajchl M, Kishimoto J, Chen Y, de Ribaupierre S, et al. 3D MR ventricle segmentation in pre-term infants with post-hemorrhagic ventricle dilatation (PHVD) using multi-phase geodesic level-sets. Neuroimage. 2015;118:13-25.
19. Krishnan P, Raybaud C, Palasamudram S, Shroff M. Neuroimaging in Pediatric Hydrocephalus. Indian J Pediatr. 2019;86(10):952-60.
20. Kline-Fath BM, Arroyo MS, Calvo-Garcia MA, Horn PS, Thomas C. Congenital aqueduct stenosis: Progressive brain findings in utero to birth in the presence of severe hydrocephalus. Prenat Diagn. 2018;38(9):706-12.
21. Eskandari R, Harris CA, McAllister JP, 2nd. Reactive astrocytosis in feline neonatal hydrocephalus: acute, chronic, and shunt-induced changes. Childs Nerv Syst. 2011;27(12):2067-76.
22. Henzi R, Guerra M, Vio K, Gonzalez C, Herrera C, McAllister P, et al. Neurospheres from neural stem/neural progenitor cells (NSPCs) of non-hydrocephalic HTx rats produce neurons, astrocytes and multiciliated ependyma: the cerebrospinal fluid of normal and hydrocephalic rats supports such a differentiation. Cell Tissue Res. 2018;373(2):421-38.
23. Paez P, Batiz LF, Roales-Bujan R, Rodriguez-Perez LM, Rodriguez S, Jimenez AJ, et al. Patterned neuropathologic events occurring in hyh congenital hydrocephalic mutant mice. J Neuropathol Exp Neurol. 2007;66(12):1082-92.
24. Jimenez AJ, Tome M, Paez P, Wagner C, Rodriguez S, Fernandez-Llebrez P, et al. A programmed ependymal denudation precedes congenital hydrocephalus in the hyh mutant mouse. J Neuropathol Exp Neurol. 2001;60(11):1105-19.
25. Date P, Ackermann P, Furey C, Fink IB, Jonas S, Khokha MK, et al. Author Correction: Visualizing flow in an intact CSF network using optical coherence tomography: implications for human congenital hydrocephalus. Sci Rep. 2020;10(1):2791.
26. Wallmeier J, Frank D, Shoemark A, Nothe-Menchen T, Cindric S, Olbrich H, et al. De Novo Mutations in FOXJ1 Result in a Motile Ciliopathy with Hydrocephalus and Randomization of Left/Right Body Asymmetry. Am J Hum Genet. 2019;105(5):1030-9.
27. Carter CS, Vogel TW, Zhang Q, Seo S, Swiderski RE, Moninger TO, et al. Abnormal development of NG2+PDGFR-alpha+ neural progenitor cells leads to neonatal hydrocephalus in a ciliopathy mouse model. Nat Med. 2012;18(12):1797-804.
28. Tabata H. Diverse subtypes of astrocytes and their development during corticogenesis. Front Neurosci. 2015;9:114.
29. Jacobsen CT, Miller RH. Control of astrocyte migration in the developing cerebral cortex. Dev Neurosci. 2003;25(2-4):207-16.
30. Del Bigio MR. Neuropathological changes caused by hydrocephalus. Acta Neuropathol. 1993;85(6):573-85.
31. Weller RO, Mitchell J. Cerebrospinal fluid edema and its sequelae in hydrocephalus. Adv Neurol. 1980;28:111-23.

32. Del Bigio MR, da Silva MC, Drake JM, Tuor UI. Acute and chronic cerebral white matter damage in neonatal hydrocephalus. Can J Neurol Sci. 1994;21(4):299-305.
33. Del Bigio MR. Cellular damage and prevention in childhood hydrocephalus. Brain Pathol. 2004;14(3):317-24.
34. Del Bigio MR, Enno TL. Effect of hydrocephalus on rat brain extracellular compartment. Cerebrospinal Fluid Res. 2008;5:12.
35. Del Bigio MR. Neuropathology and structural changes in hydrocephalus. Dev Disabil Res Rev. 2010;16(1):16-22.
36. Gosztonyi G, Ludwig H, Bode L, Kao M, Sell M, Petrusz P, et al. Obesity induced by Borna disease virus in rats: key roles of hypothalamic fast-acting neurotransmitters and inflammatory infiltrates. Brain Struct Funct. 2020;225(5):1459-82.
37. Shook BA, Lennington JB, Acabchuk RL, Halling M, Sun Y, Peters J, et al. Ventriculomegaly associated with ependymal gliosis and declines in barrier integrity in the aging human and mouse brain. Aging Cell. 2014;13(2):340-50.
38. Xiong G, Elkind JA, Kundu S, Smith CJ, Antunes MB, Tamashiro E, et al. Traumatic brain injury-induced ependymal ciliary loss decreases cerebral spinal fluid flow. J Neurotrauma. 2014;31(16):1396-404.
39. Verkhratsky A, Nedergaard M. Physiology of Astroglia. Physiol Rev. 2018;98(1):239-389.
40. Pikor NB, Cupovic J, Onder L, Gommerman JL, Ludewig B. Stromal Cell Niches in the Inflamed Central Nervous System. J Immunol. 2017;198(5):1775-81.
41. Baburamani AA, Vontell RT, Uus A, Pietsch M, Patkee PA, Wyatt-Ashmead J, et al. Assessment of radial glia in the frontal lobe of fetuses with Down syndrome. Acta Neuropathol Commun. 2020;8(1):141.
42. Liddelow SA, Guttenplan KA, Clarke LE, Bennett FC, Bohlen CJ, Schirmer L, et al. Neurotoxic reactive astrocytes are induced by activated microglia. Nature. 2017;541(7638):481-7.
43. Miller SJ. Astrocyte Heterogeneity in the Adult Central Nervous System. Front Cell Neurosci. 2018;12:401.
44. Bayraktar OA, Fuentealba LC, Alvarez-Buylla A, Rowitch DH. Astrocyte development and heterogeneity. Cold Spring Harb Perspect Biol. 2014;7(1):a020362.
45. Liddelow SA, Barres BA. Reactive Astrocytes: Production, Function, and Therapeutic Potential. Immunity. 2017;46(6):957-67.
46. Li T, Chen X, Zhang C, Zhang Y, Yao W. An update on reactive astrocytes in chronic pain. J Neuroinflammation. 2019;16(1):140.
47. Mrozek S, Delamarre L, Capilla F, Al-Saati T, Fourcade O, Constantin JM, et al. Cerebral Expression of Glial Fibrillary Acidic Protein, Ubiquitin Carboxy-Terminal Hydrolase-L1, and Matrix Metalloproteinase 9 After Traumatic Brain Injury and Secondary Brain Insults in Rats. Biomark Insights. 2019;14:1177271919851515.

48. Yang T, Dai Y, Chen G, Cui S. Dissecting the Dual Role of the Glial Scar and Scar-Forming Astrocytes in Spinal Cord Injury. Front Cell Neurosci. 2020;14:78.
49. Wang H, Song G, Chuang H, Chiu C, Abdelmaksoud A, Ye Y, et al. Portrait of glial scar in neurological diseases. Int J Immunopathol Pharmacol. 2018;31:2058738418801406.
50. Ribotta MG, Menet V, Privat A. Glial scar and axonal regeneration in the CNS: lessons from GFAP and vimentin transgenic mice. Acta Neurochir Suppl. 2004;89:87-92.
51. Wanner IB, Anderson MA, Song B, Levine J, Fernandez A, Gray-Thompson Z, et al. Glial scar borders are formed by newly proliferated, elongated astrocytes that interact to corral inflammatory and fibrotic cells via STAT3-dependent mechanisms after spinal cord injury. J Neurosci. 2013;33(31):12870-86.
52. Ringstad G, Vatnehol SAS, Eide PK. Glymphatic MRI in idiopathic normal pressure hydrocephalus. Brain. 2017;140(10):2691-705.
53. Rosenberg GA, Kyner WT, Estrada E. The effect of increased CSF pressure on interstitial fluid flow during ventriculocisternal perfusion in the cat. Brain Res. 1982;232(1):141-50.
54. Bradley WG, Jr. Diagnostic tools in hydrocephalus. Neurosurg Clin N Am. 2001;12(4):661-84, viii.
55. Del Bigio MR, Slobodian I, Schellenberg AE, Buist RJ, Kemp-Buors TL. Magnetic resonance imaging indicators of blood-brain barrier and brain water changes in young rats with kaolin-induced hydrocephalus. Fluids Barriers CNS. 2011;8:22.
56. Mangano FT, McAllister JP, 2nd, Jones HC, Johnson MJ, Kriebel RM. The microglial response to progressive hydrocephalus in a model of inherited aqueductal stenosis. Neurol Res. 1998;20(8):697-704.
57. Eskandari R, Abdullah O, Mason C, Lloyd KE, Oeschle AN, McAllister JP, 2nd. Differential vulnerability of white matter structures to experimental infantile hydrocephalus detected by diffusion tensor imaging. Childs Nerv Syst. 2014;30(10):1651-61.
58. Oberheim NA, Goldman SA, Nedergaard M. Heterogeneity of astrocytic form and function. Methods Mol Biol. 2012;814:23-45.
59. Miller RH, Raff MC. Fibrous and protoplasmic astrocytes are biochemically and developmentally distinct. J Neurosci. 1984;4(2):585-92.
60. Ikeshima-Kataoka H. Neuroimmunological Implications of AQP4 in Astrocytes. Int J Mol Sci. 2016;17(8).
61. Saadoun S, Papadopoulos MC, Watanabe H, Yan D, Manley GT, Verkman AS. Involvement of aquaporin-4 in astroglial cell migration and glial scar formation. J Cell Sci. 2005;118(Pt 24):5691-8.
62. Ciappelloni S, Bouchet D, Dubourdieu N, Boue-Grabot E, Kellermayer B, Manso C, et al. Aquaporin-4 Surface Trafficking Regulates Astrocytic Process Motility and Synaptic Activity in Health and Autoimmune Disease. Cell Rep. 2019;27(13):3860-72 e4.
63. Ding T, Ma Y, Li W, Liu X, Ying G, Fu L, et al. Role of aquaporin-4 in the regulation of migration and invasion of human glioma cells. Int J Oncol. 2011;38(6):1521-31.

64. Eilert-Olsen M, Hjukse JB, Thoren AE, Tang W, Enger R, Jensen V, et al. Astroglial endfeet exhibit distinct Ca(2+) signals during hypoosmotic conditions. Glia. 2019;67(12):2399-409.
65. Shandra O, Winemiller AR, Heithoff BP, Munoz-Ballester C, George KK, Benko MJ, et al. Repetitive Diffuse Mild Traumatic Brain Injury Causes an Atypical Astrocyte Response and Spontaneous Recurrent Seizures. J Neurosci. 2019;39(10):1944-63.

# Figures

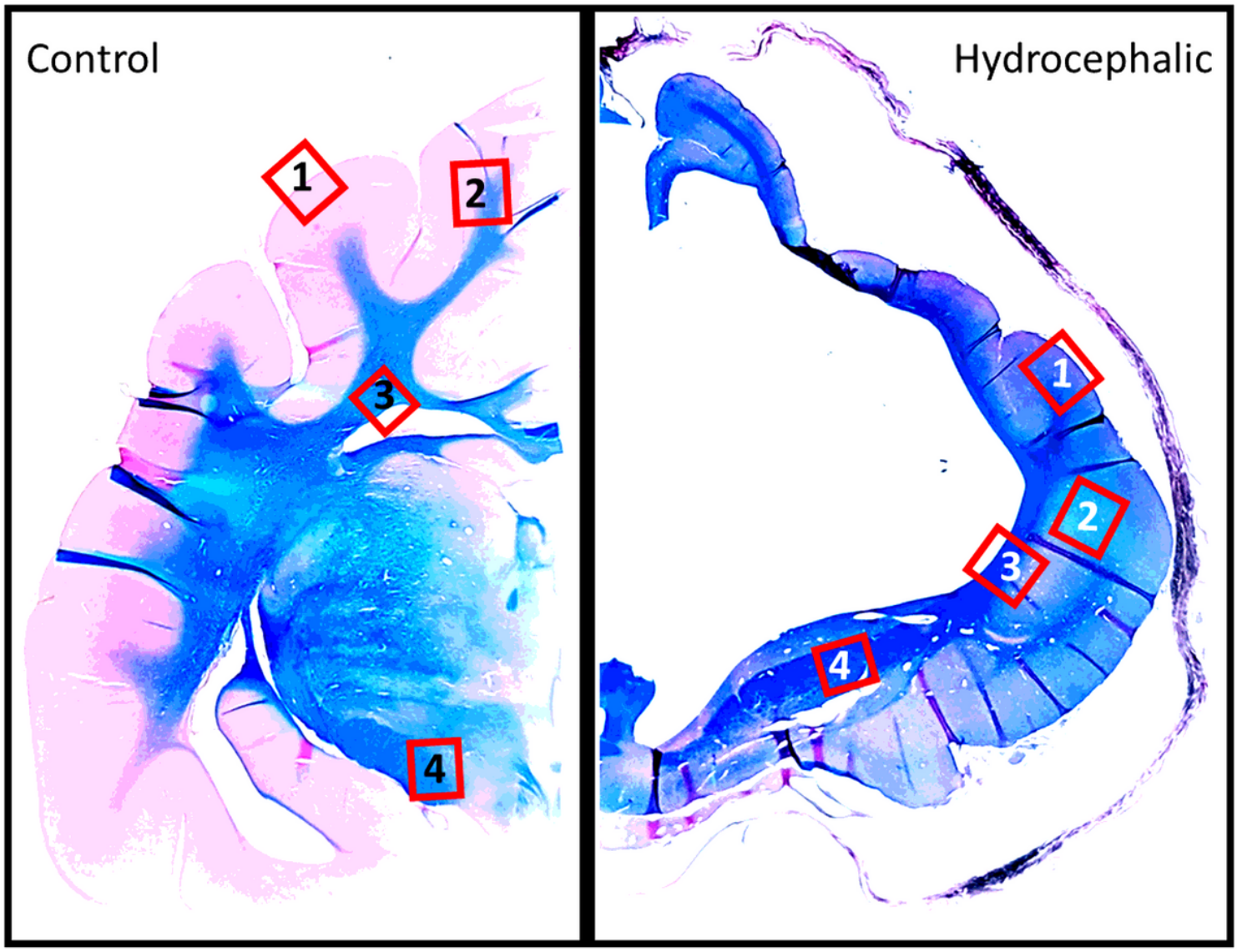


**Figure 1**

Representative histological Luxol Fast Blue (LFB) with Hematoxylin & Eosin (H/E) staining of control (right) and hydrocephalic (left) coronal sections demonstrating regions of interest (ROI) obtained for quantitative densitometry. ROI-1 = Superficial Cortex; ROI-2 = Deep Cortex; ROI-3 = Periventricular; ROI-4 = Deep White Matter; V = ventricle, ar = arachnoid

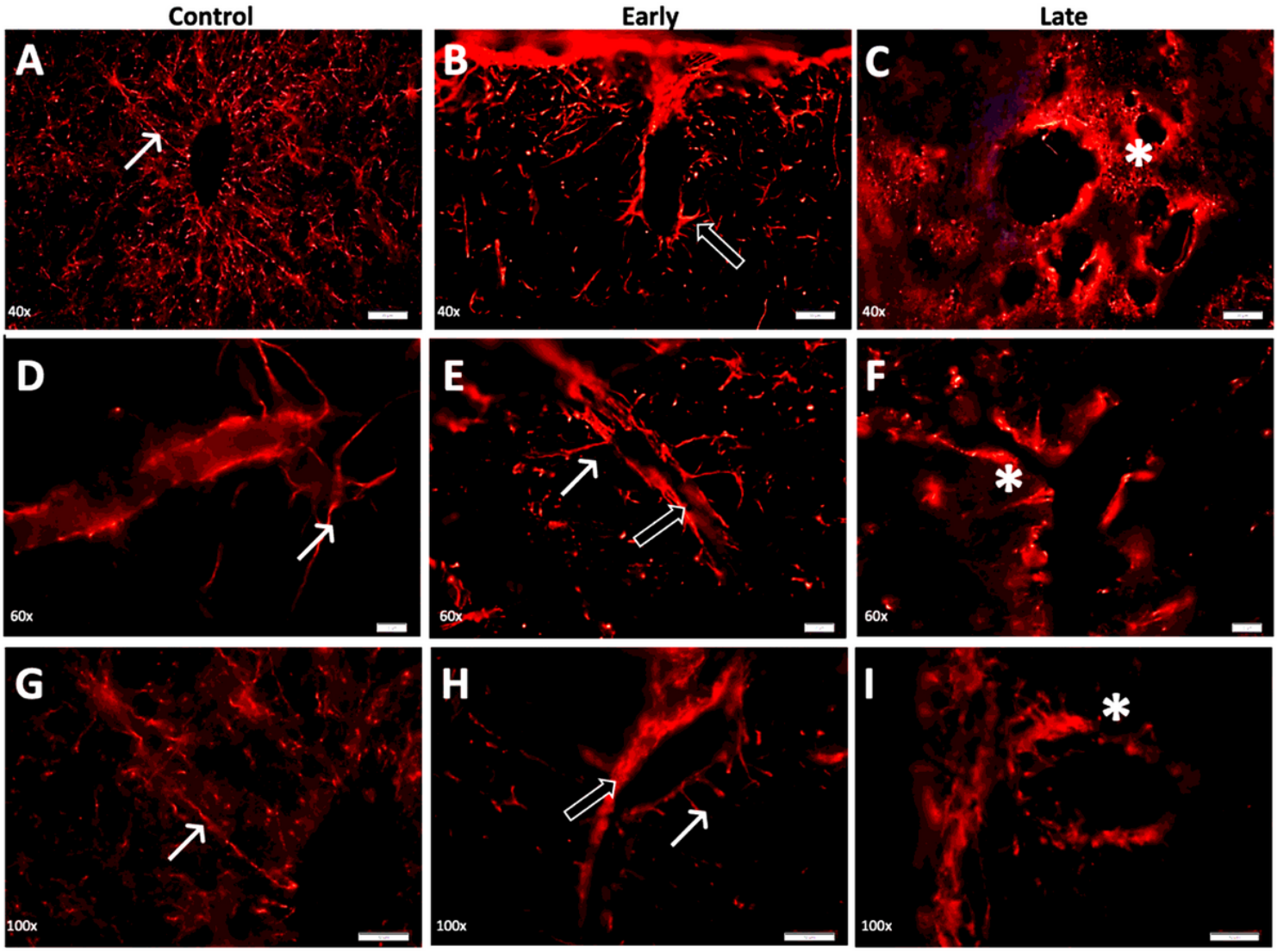


## Figure 2

High-powered immunofluorescence photographs of medium-sized microvasculature within the deep parietal cortex of control (A, D, G), early-treated reservoir (B, E, H) and late-treated (C, F, I) animals. Comparatively, individual astrocytic endfeet can be seen terminating on the vessel surface in controls (thin arrow), demonstrating typical relationships of non-reactive astrocytes and parenchymal microvasculature. Note the non-GFAP staining between the astrocytic endfeet termini on the vessel surface (thin arrow). GFAP+ perivascular gliotic scar formation in both early-treated and late-treated hydrocephalic animals is noted (black arrow). Early-treated group vasculature (B, E, H) demonstrate decreased total identifiable end-feet with increased thickness of GFAP+ staining. Vasculature from the late-treated group demonstrates further paucity of healthy astrocytes and significantly increased GFAP+ gliosis and scar formation (*).

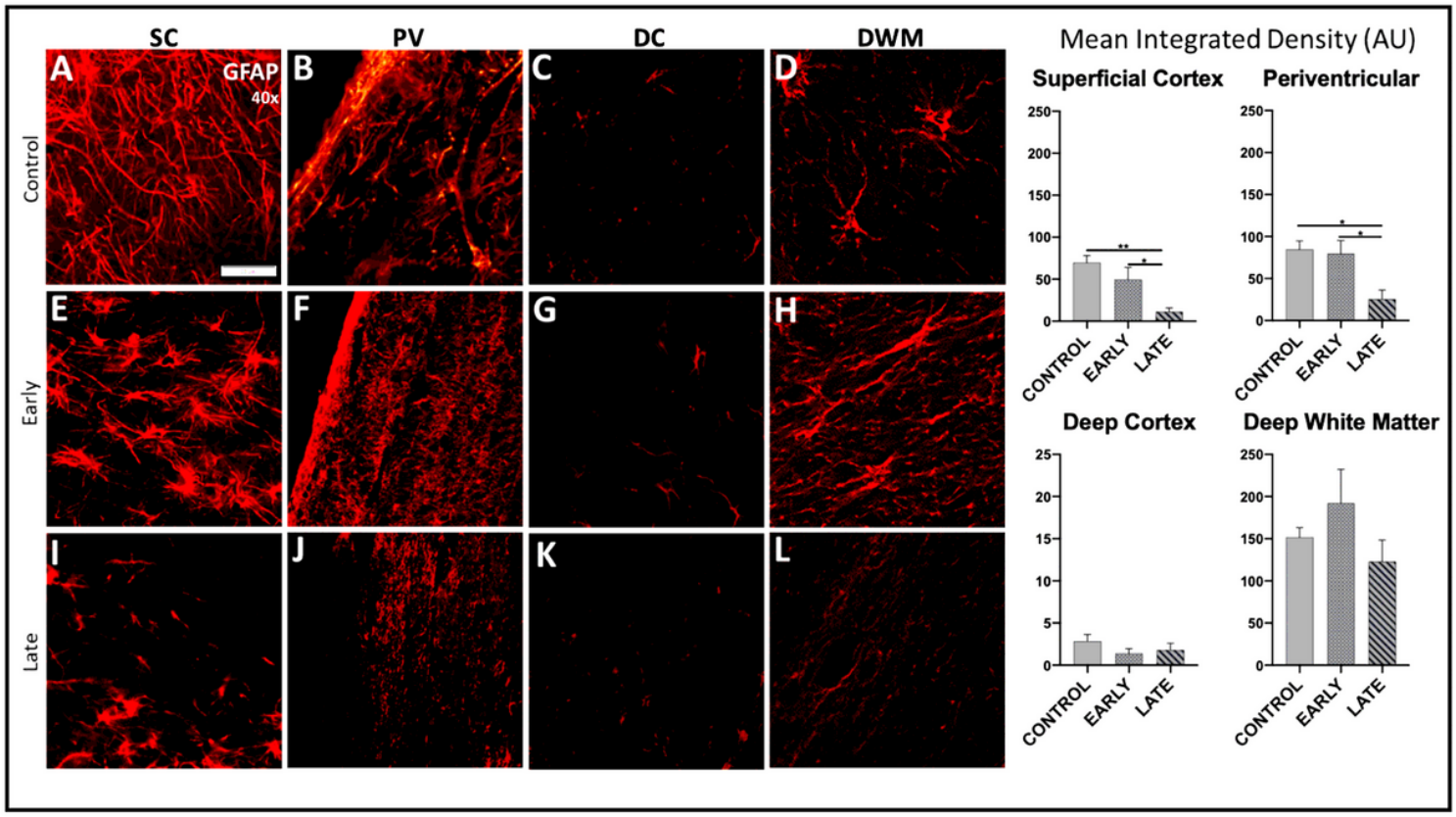


## Figure 3

Immunofluorescent micrographs depicting GFAP expression within four regions of interest of experimental animals (Control, Early and Late). Regions of Control group superficial cortex (SC) demonstrate thin, elongated GFAP+ processes with consistent morphological appearance of astrocyte cell bodies (A). Astrocytes within this same region of the Early treatment groups exhibit hypertrophic cell bodies and decreased staining of GFAP+ process (E). Identifiable astrocytes within the SC of the Late treatment group were scarce and GFAP+ staining was morphologically characteristic of reactive astrocytes. Similar patterns were observed across the periventricular (B, F, J), deep cortex (C, G ,K) and deep white matter regions (D, H, L). Each graph shows relative GFAP levels within each region of the respective cohort. SC-superficial cortex; PV-periventricular; DC-deep cortex; DWM-deep white matter.

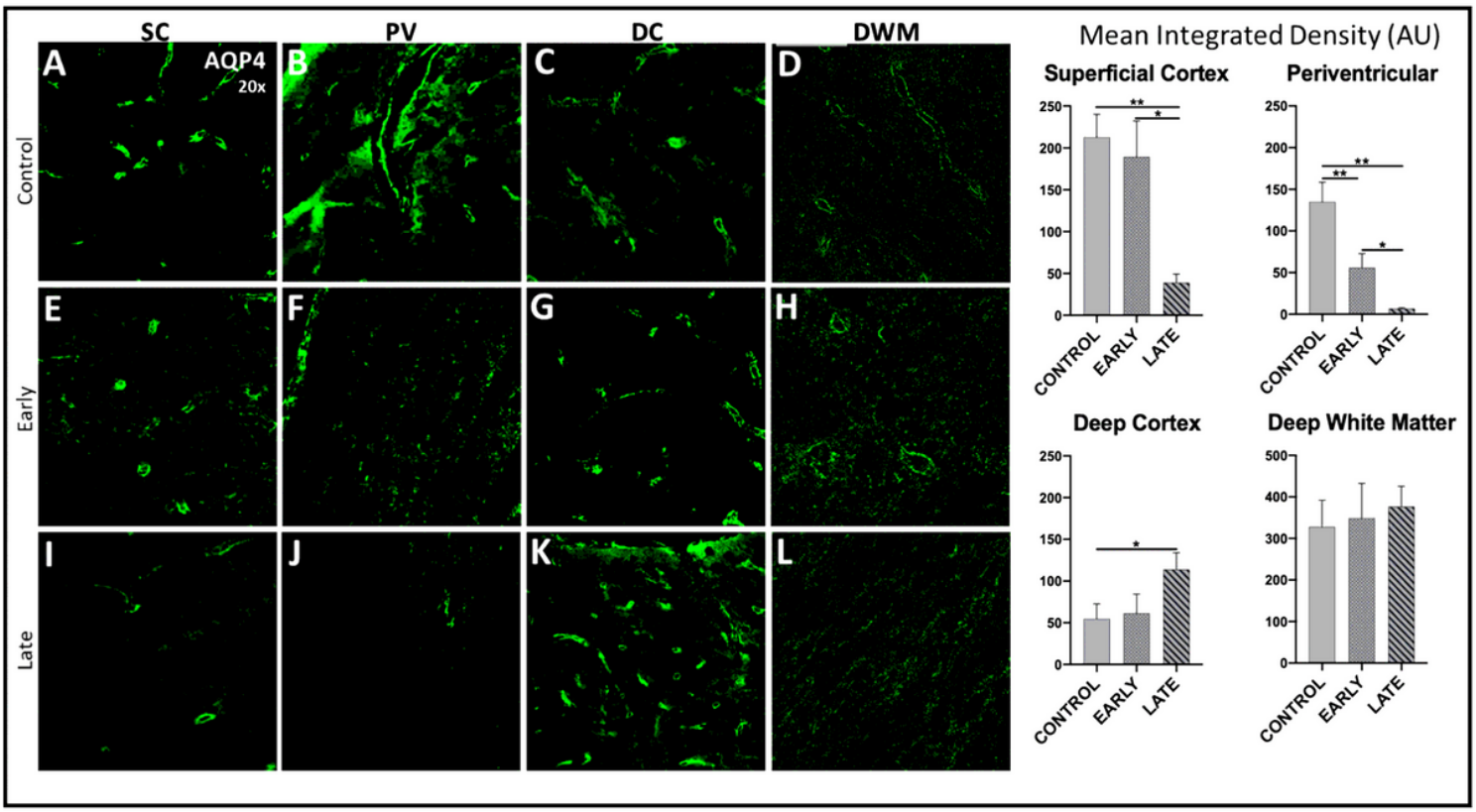


## Figure 4

Immunofluorescent micrographs depicting AQP4 expression within four regions of interest of experimental animals (Control, Early and Late). Prominent AQP4 localization is seen along the perivascular boundary of superficial cortex (SC) region vessels of Control animals (A, B, C, D). Non-specific AQP4 staining is observed following hydrocephalus mediated injury, and is apparent in the SC, PV and DWM regions of both Early and Late treatment group animals (Early: E, F, H; Late: I, J, L). Within the DC region of Early and Late treatment groups, chronic injury led to increased perivascular AQP4 localization. Each graph shows relative AQP4 levels within each region of the respective cohort. SC-superficial cortex; PV-periventricular; DC-deep cortex; DWM-deep white matter.

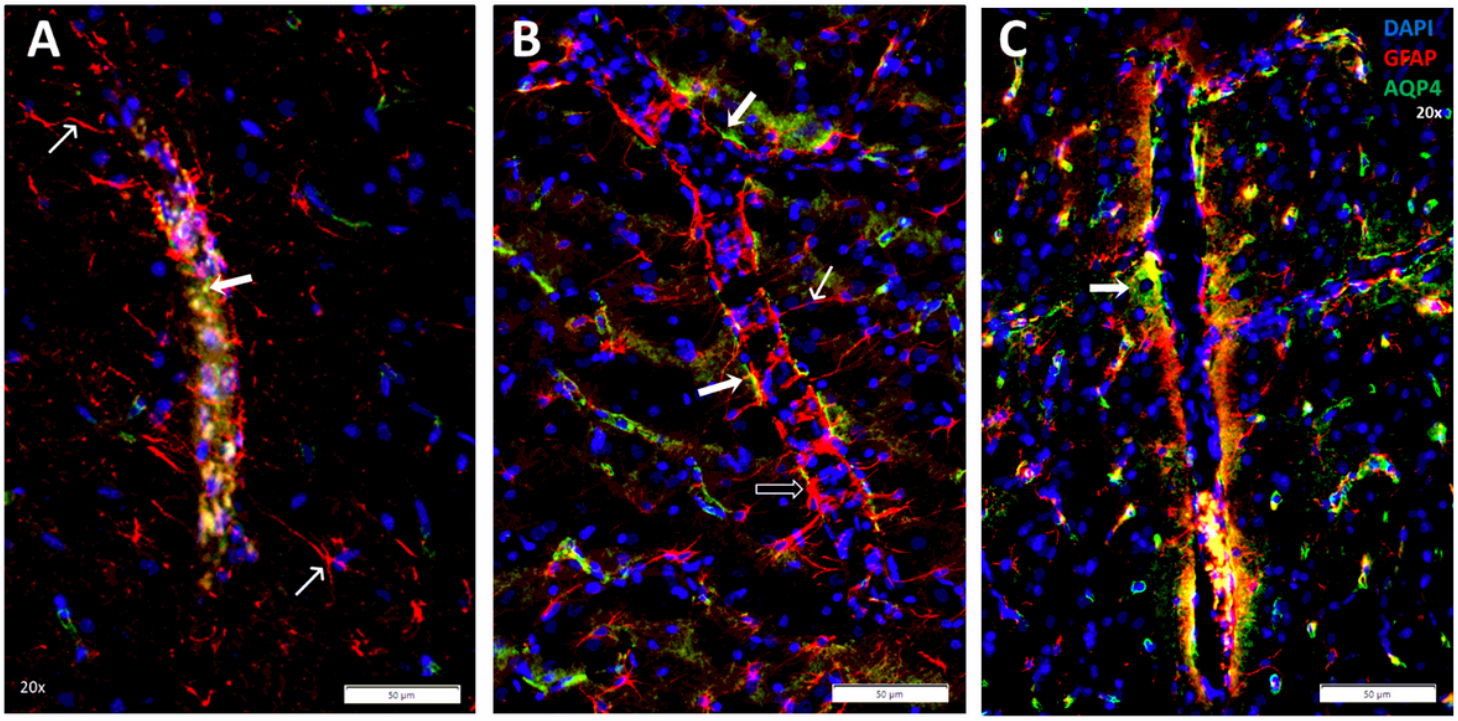


**Figure 5**

Immunohistochemical photographs of deep cortex microvasculature of parietal lobe in Control (A), Early-treated reservoir treated (B) and Late-treated (C) animals. Reactive astrocytes with endfeet terminate on microvessels (thin white arrow) in Controls, unlike reactive astrocytes (black arrow) with shorter processes in Early-treated hydrocephalic animals and almost complete loss of discernable astrocytes surrounding vessels in Late-treated animals. The surrounding microvascular environment demonstrates an increase in AQP-4 (thick white arrow) in both early-treated and late-treated groups. Scale bar = 50µm, 20x magnification.

## Supplementary Files

This is a list of supplementary files associated with this preprint. Click to download.

- SupplementalFigure1.png